

Chapter 7

Studies of the 2D Silicide Surface

7.1 Introduction

Two dimensional rare earth silicides have been seen to be novel and interesting structures. Their unusual properties may lead to technological applications. The crystallographic structure of these 2D silicides is now well known [1-7], and detailed study as described in Chapter 5 has revealed trends in this structure across the series. It is timely and interesting to study the electronic structure of these surfaces as well as investigating the interaction of this interface with further metallic overlayers.

Preliminary experiments along these lines have been performed. The first section of this chapter discusses an investigation of the electronic structure of the 2D silicide surface on the atomic scale by means of scanning tunnelling spectroscopy (STS). The second section describes an initial look at the possibility of using the unusual 1×1 surface as a novel growth template, in this case for the formation of Fe silicide.

7.2 STS of 2D Holmium Silicide

7.2.1 Introduction

Two dimensional Ho silicide has a structure extremely similar to that of the two dimensional Tm silicide, as discussed in Chapters 4 and 5. The structure has been well studied [2, 8, 9]. The electronic structure of similar 2D rare earth silicides has been investigated by a number of groups [4, 9-16]. Unsurprisingly given the similarities between rare earth metals and the structure of all these silicides, few differences have been observed in the electronic structure. The band structure

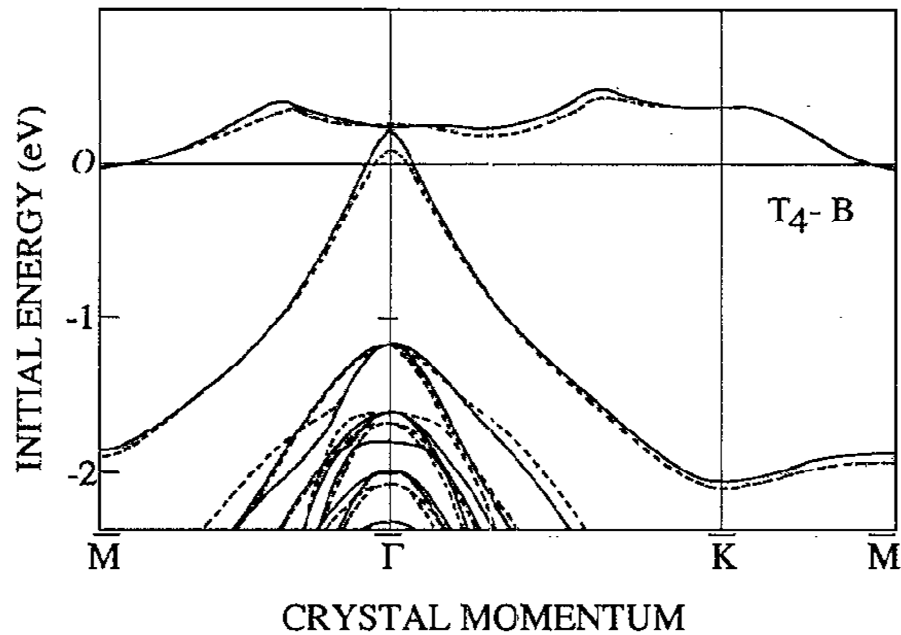


Figure 7.1: Theoretical band structure of RE 2D silicide [4]. Note the hole pocket at the $\bar{\Gamma}$ point.

(Figure 7.1) shows an interesting hole pocket at the Γ -point and electron pocket around the M-point. There is an occupied state approximately 1.3eV below the Fermi energy at the Γ -point and a flat band just above the Fermi energy.

Of the three rare earth valence electrons one saturates the upward pointing dangling bond of the Si bilayer beneath and a second the downward pointing dangling bonds of that above. The third valence electron forms a fairly delocalised 5d–3p hybridised state with the Si of the top bilayer.

7.2.2 Experimental

The STM and STS results reported here were obtained using the Omicron STMs described in Chapter 2. Si(111) samples were cut from lightly doped 100 Ω cm *n*-type wafers. The base pressure of the UHV systems was around 1×10^{-10} mbar. The samples were cleaned by passing direct current through them to repeatedly flash heat to ~ 1200 $^{\circ}\text{C}$ with slow cooling (< 100 $^{\circ}\text{C}/\text{min}$) to room temperature. The cleanliness of the surface was confirmed by the characteristic sharp 7×7 LEED pattern. Ho was deposited at room temperature onto the freshly prepared

sample from a homemade source similar to that used for the deposition of Tm in Chapter 4. The as deposited samples produced only a diffuse background when examined with LEED. Samples were annealed to about 500 °C by passing direct current through them, the temperature being measured using an external infra-red pyrometer. After anneal a sharp, low background 1×1 LEED pattern was observed and was taken to indicate the successful formation of a 2D Ho silicide. Samples were then transferred under UHV conditions to the STM instrument and probed using chemically etched tungsten tips.

7.2.3 Scanning Tunnelling Microscopy

The principles of STM and STS have been described in Chapter 2. STM was performed on the 2D Ho silicides, with atomic resolution. STM images of the surface of the 2D silicide reveal the 1×1 reconstruction of the uppermost Si bilayer. Figure 7.2 and Figure 7.3 show typical images. Figure 7.3 indicates several inequivalent sites on the surface. On Top indicates sites directly above the uppermost Si atom. Dark A and DarkB represent those sites located above the RE atoms (H3 sites) or above the lower Si atom of the terminating Si bilayer (T4 sites). Unfortunately there is no way to distinguish if Dark A corresponds to the former case (in which case Dark B would be above the Si) or the latter (in which case DarkB would be above the RE) from the STM image alone.



Figure 7.2: Atomically resolved STM image of the 2D Ho silicide surface. Imaged acquired at a bias voltage of 2V, tunnelling current 2nA. ~ 10 nm \times ~ 3 nm.

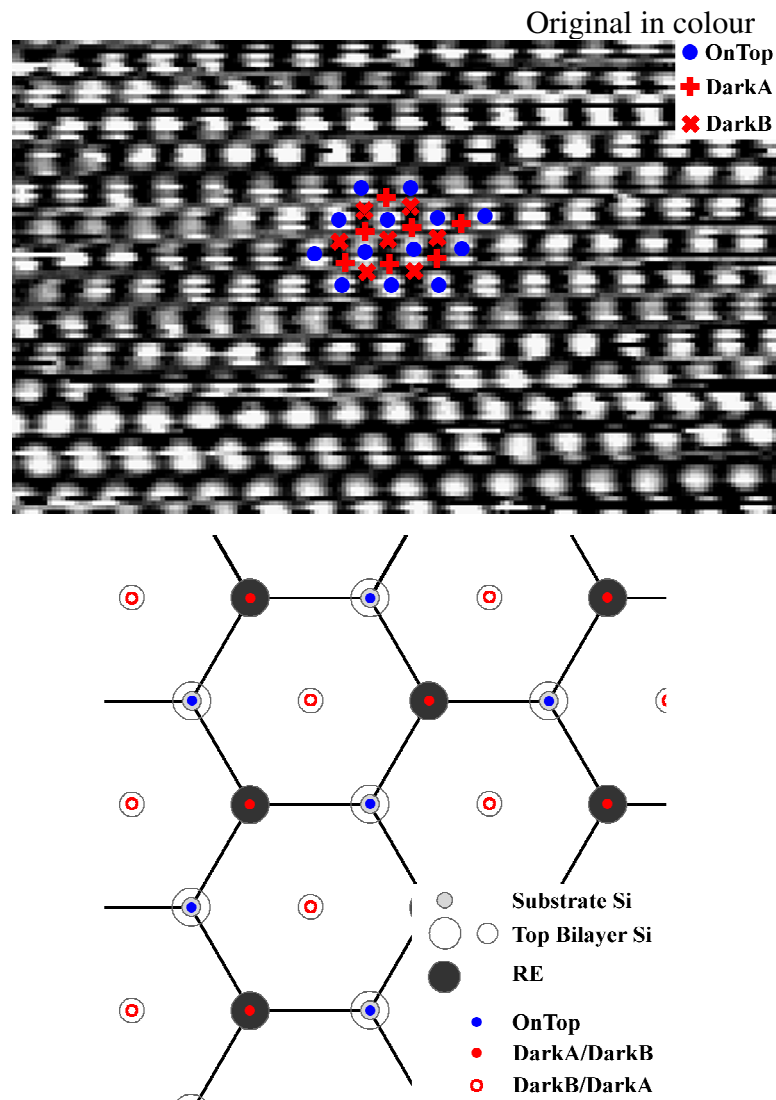


Figure 7.3: Inequivalent sites on the 2D silicide surface. Top: atomically resolved STM image, bias voltage 2 V, tunnelling current 2 nA. ~ 5.0 nm \times ~ 3.6 nm. Bottom: Schematic top view of the surface.

7.2.4 Scanning Tunnelling Spectroscopy

Scanning tunnelling spectroscopy curves were obtained at a regular grid of points whilst performing atomic resolution STM of the 2D Ho silicide. A typical plot of tunnelling current versus applied bias voltage is shown in Figure 7.4. It is well established [17-19] that a plot of the logarithmic derivative of the tunnelling current, $(dI/dV)/(I/V)$ —or equivalently $d[\ln(I)]/d[\ln(V)]$ —, produces a good representation of the local density of states. This quantity removes the

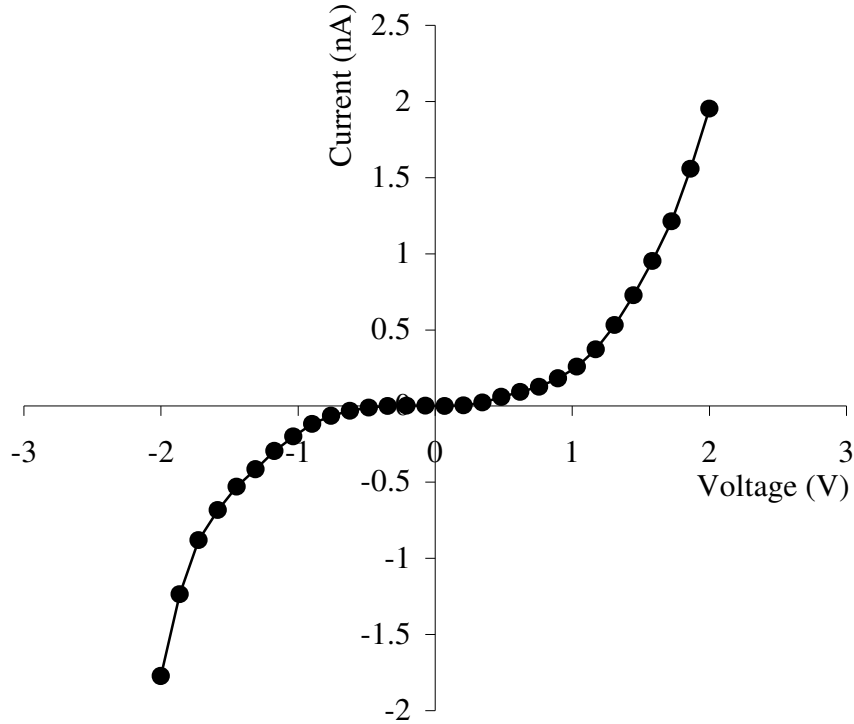


Figure 7.4: Typical plot of tunnelling current, I , versus bias voltage, V , averaged from equivalent sites on the atomically resolved 2D silicide surface close to zero applied voltage.

dependence of the tunnelling current on the sample–tip separation. Such a plot ~derived from the curve of Figure 7.4 is shown in Figure 7.5. It is noted that in practice the I/V curve is often noisy in the low voltage regime ($\sim -0.3 \text{ V} \leq V \leq \sim +0.3 \text{ V}$). This can result in spurious large peaks in the logarithmic derivative. To prevent this problem the I/V curve is broadened by convoluting it with a response function of the form $\exp(-|V/\Delta V|)$, i.e.

$$\overline{I/V} = (I/V) e^{-|V/\Delta V|} \quad (7.1)$$

The term ΔV gives the width of the broadening function and must be chosen so as to be small enough not to wash out all detail while remaining large enough to remove the spurious noise. A value of $\Delta V = 0.66 \text{ V}$ has been found to give

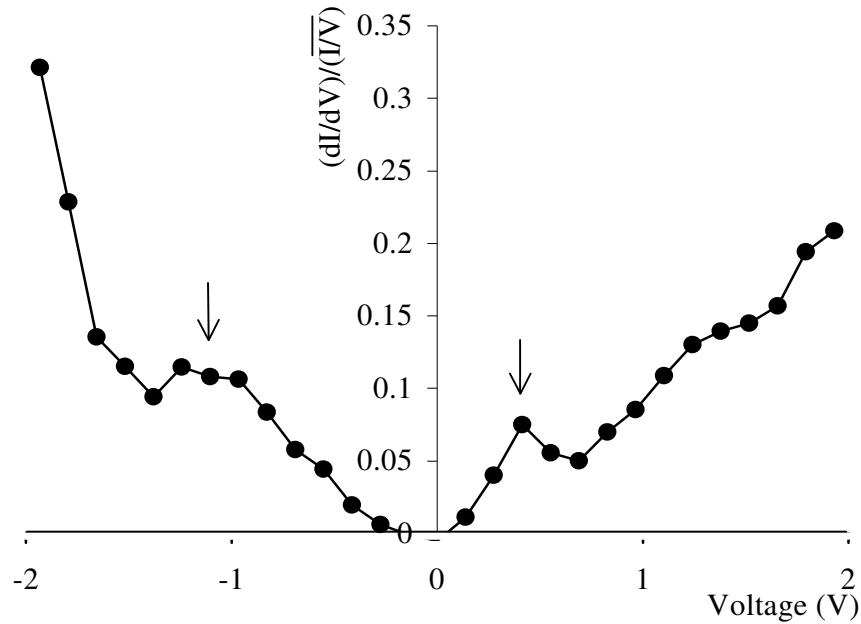


Figure 7.5: The LDOS is better represented by a plot of $(dI/dV)/(I/V)$ versus bias voltage. Arrowed are features corresponding to bands in the 2D silicide band structure

satisfactory results [20]. It is this value which is used in the calculation of the logarithmic derivatives [19-21].

7.2.5 Spatially Resolved Spectra

STS spectra were obtained over a grid of points on a spatially resolved STM image. Three inequivalent sites were identified as indicated in Figure 7.3. For each of these sites the I/V curves from many equivalent points were averaged to give a final I/V curve and the logarithmic derivative calculated. The results of this exercise may be seen in Figure 7.6. It is immediately apparent that the spectra from each site are indistinguishable within error. This is unusual and in stark contrast to a surface such as the Si(111) 7×7 reconstruction where inequivalent sites show a clear difference in the STS spectra obtained [22-24]. Figure 7.7 shows STS collected from a region of 2D silicide imaged alongside a region of Si(111) 7×7 . The different sites within the 7×7 unit cell can be distinguished and are in reasonable agreement with published results [22-24].

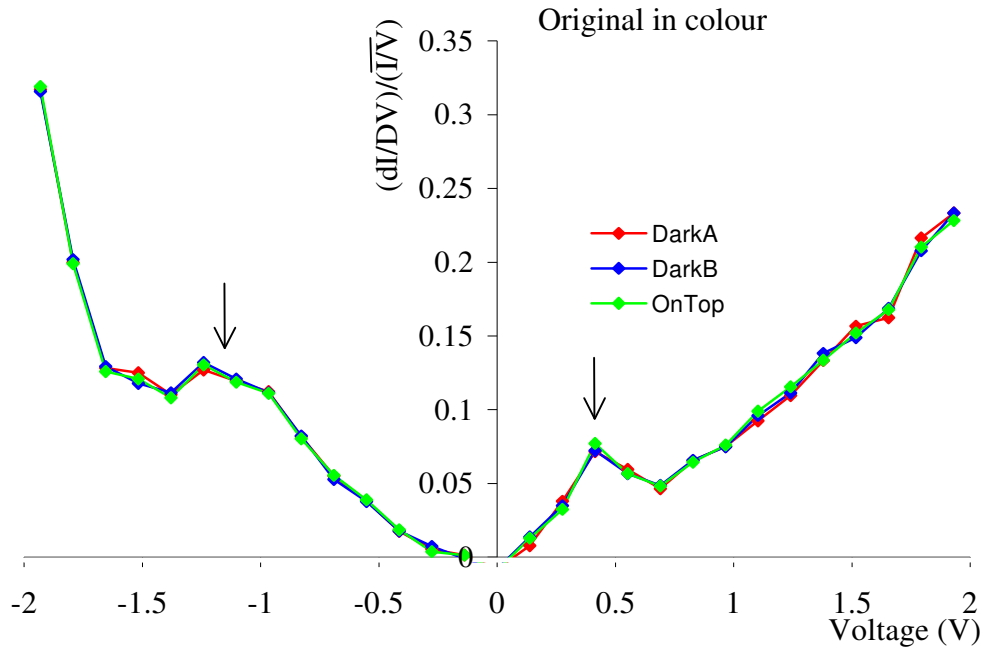


Figure 7.6: STS spectra from three inequivalent sites on the atomically resolved 2D Ho silicide surface. Arrowed are features corresponding to bands in the 2D silicide band structure.

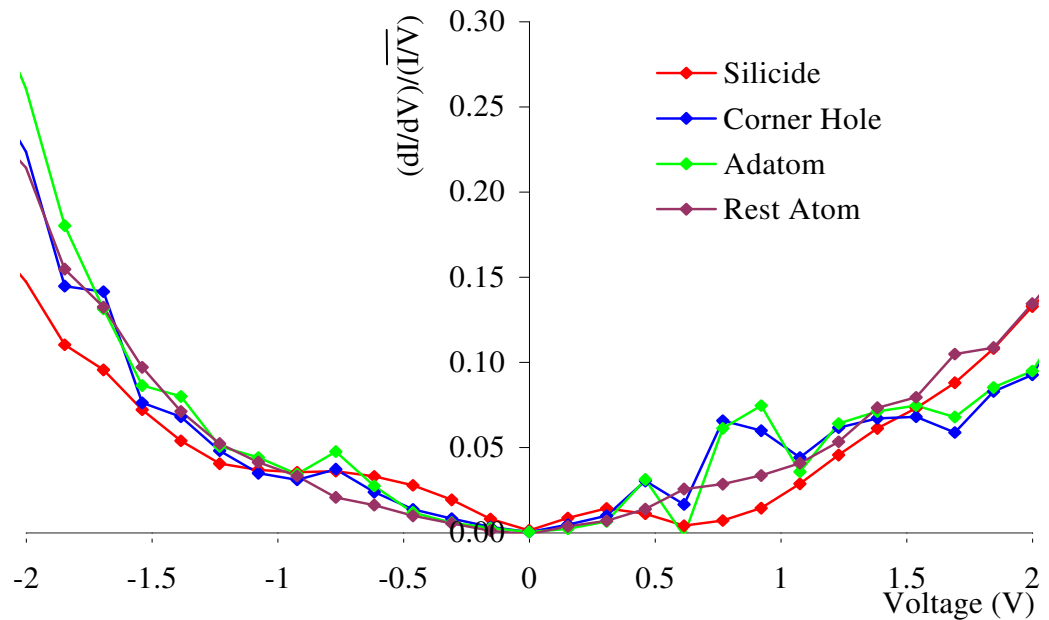


Figure 7.7: Comparison of STS from a region of 2D silicide and various sites within the Si(111) 7×7 unit cell.

This suggests that the tip electronic structure is having a negligible effect on the spectroscopy obtained.

The spectra obtained may be understood in terms of the band structure of 2D silicides. Although the experiments reported here involved Ho silicides theoretical and experimental band structures for other 2D silicides have been reported [4, 13, 16]. It is expected that the band structure in the Ho case will be very similar.

The states mainly involved with tunnelling will be those for which k_{\parallel} is small, i.e. those around the Γ -point of the surface Brillouin zone. As mentioned above the states around the Γ -point are formed by the hybridisation of the rare earth 5d and top layer Si dangling bond 3d states and are hence fairly delocalised. It is this delocalisation which means individual sites are so difficult to distinguish in the case of the Ho silicide. This delocalisation has previously been noted in the case of the so called 3D silicide formed at higher coverage [25]. As there, here it seems that the STM image closely reflects the actual topography of the sample.

The occupied state band at ~ -1.3 eV is observed in the STS as is the empty state band ~ 0.5 eV above the Fermi level (indicated by arrows in Figure 7.6).

Although the precise bias voltage at which these features occur is seen to move slightly between samples (probably due to band bending and other tip-sample interactions—spectra taken with a higher current set-point tend to show the features at higher bias voltage) they consistently appear across spectra taken from a range of samples and with numerous tips. In fact STS offers one of the few ways to experimentally access the band structure above the Fermi level and confirm the theoretical predictions (at least around the Γ -point).

7.3 Initial MEIS Study of Fe Growth on 2D Holmium Silicide

7.3.1 Introduction

It has previously been mentioned that it is possible 2D rare earth silicides may find technological applications. The possibility of the rare earth layer acting as a barrier for a role in spin electronics was mentioned in Chapter 6. It is important to understand how this novel surface interacts with metallic overlayers. As an initial approach to the investigation of this problem a brief MEIS study of the growth of Fe on the surface of a Ho 2D silicide was undertaken. MEIS offers an ideal tool for the study of the crystallography of any interface at the surface of these systems. The rare earth signal may be extracted and analysed to give information about atomic positions of those layers closer to the surface. If the deposited metal is also well separated in mass from the Si and rare earth then the signal from all three elements may be observed. This is the case with Fe.

7.3.2 Experimental

The experiments were carried out at the Daresbury MEIS facility, previously described in Chapter 2. Samples were prepared in a similar manner to the Tm 2D silicides discussed in Chapter 4. One monolayer of Ho was deposited onto the freshly prepared Si(111) 7×7 surface and annealed to ~ 550 °C. The formation of a 2D silicide was confirmed by the sharp 1×1 LEED pattern and the characteristic blocking features. Note the clear blocking feature visible in the spectrum from the 2D silicide shown in Figure 7.8 and Figure 7.9 insets.

Fe was deposited from a source of similar design to that used in the experiments of Chapter 6. The Fe coverage was estimated from the MEIS spectra to be 1.7 ML. Immediately after the Fe deposition the 1×1 LEED pattern was seen to no longer be present with only a diffuse background observed. The sample was transferred under UHV to the MEIS scattering chamber and a series of MEIS

spectra taken.

7.3.3 *Results and Discussion*

The MEIS spectra from the as-deposited, room temperature Fe/Si(111) 1×1 -Ho sample is shown in Figure 7.8a. The scattering signals from all three elements are clearly resolved. A small oxygen signal, (just visible in Figure 7.8b), was also detected. The uncorrected (for Rutherford scattering cross-section and TEA offset) scattering curves from the Ho and Fe signals are shown in Figure 7.9a. As this was a preliminary investigation only one data set was available and the scattering curves are hence noisier than might have been desired. Never the less, it is still clear that there are no major blocking features in any of the Fe, Ho or Si signals, indicating that the Fe has not formed an ordered structure and has disrupted the structure of the 2D silicide.

The sample was further annealed to around 550 °C. The MEIS spectra shown in Figure 7.8b was taken after this anneal. The broadening of the Fe scattering signal indicates that the Fe is beginning to diffuse into the bulk. The slight broadening of the Ho scattering signal is probably due to intermixing of the Fe and Ho. The scattering curves from this system are shown in Figure 7.9b. Again although noisy the scattering curves clearly lack the blocking features expected from an ordered surface.

The sample was annealed yet further to ~700 °C. This succeeded only in causing the Ho and Fe to both completely diffuse into the bulk, as shown by Figure 7.8c. Throughout the annealing sequence there was no LEED pattern detectable, only a bright, diffuse background, confirming the lack of ordered surface structure.

Original in colour

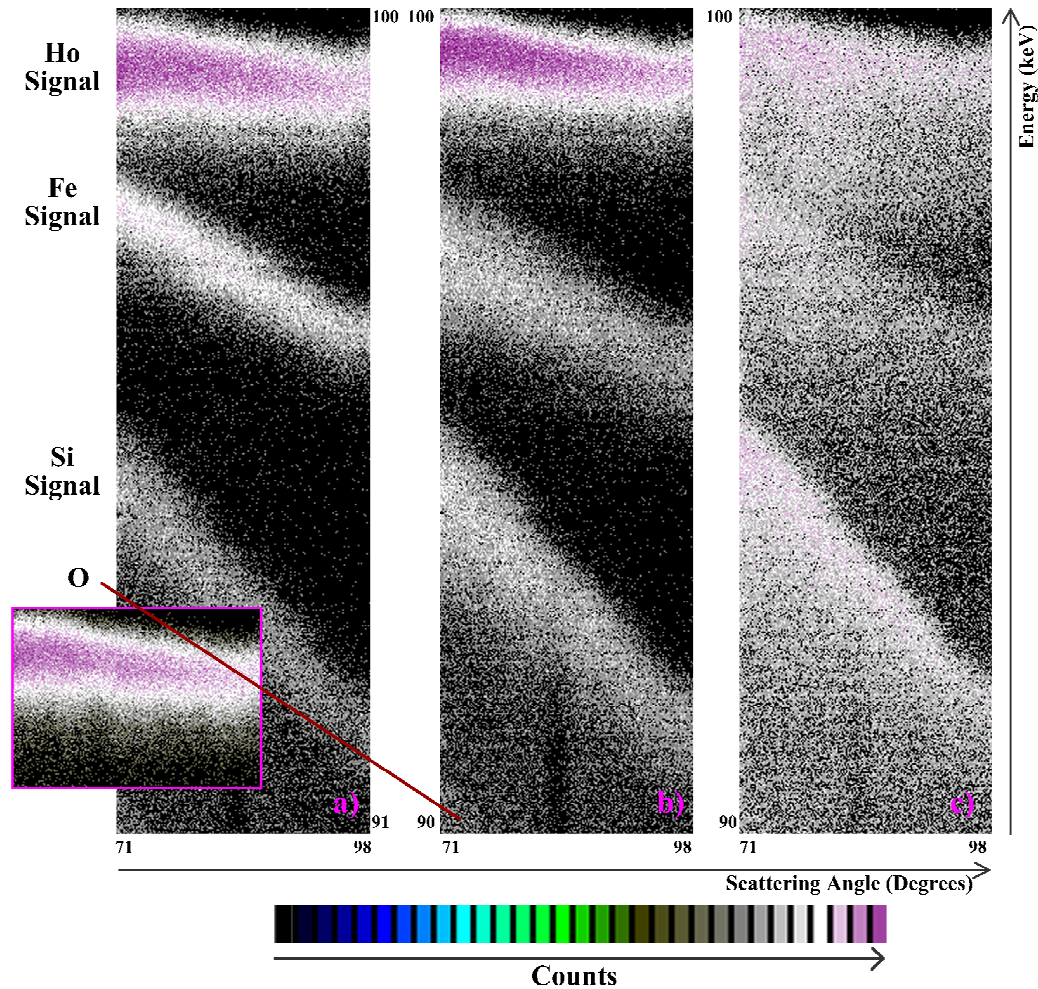


Figure 7.8: The sequence of MEIS spectra from Fe deposition on Ho 2D silicide. $[1\bar{1}0]$ incident direction with detection around $[100]$. a) As deposited b) After anneal to ~ 550 °C c) After anneal to ~ 700 °C. The inset shows the Ho scattering signal from the 2D silicide before Fe deposition. The surface is initially disrupted and increasing annealing simply causes diffusion of the Fe and Ho into the bulk substrate.

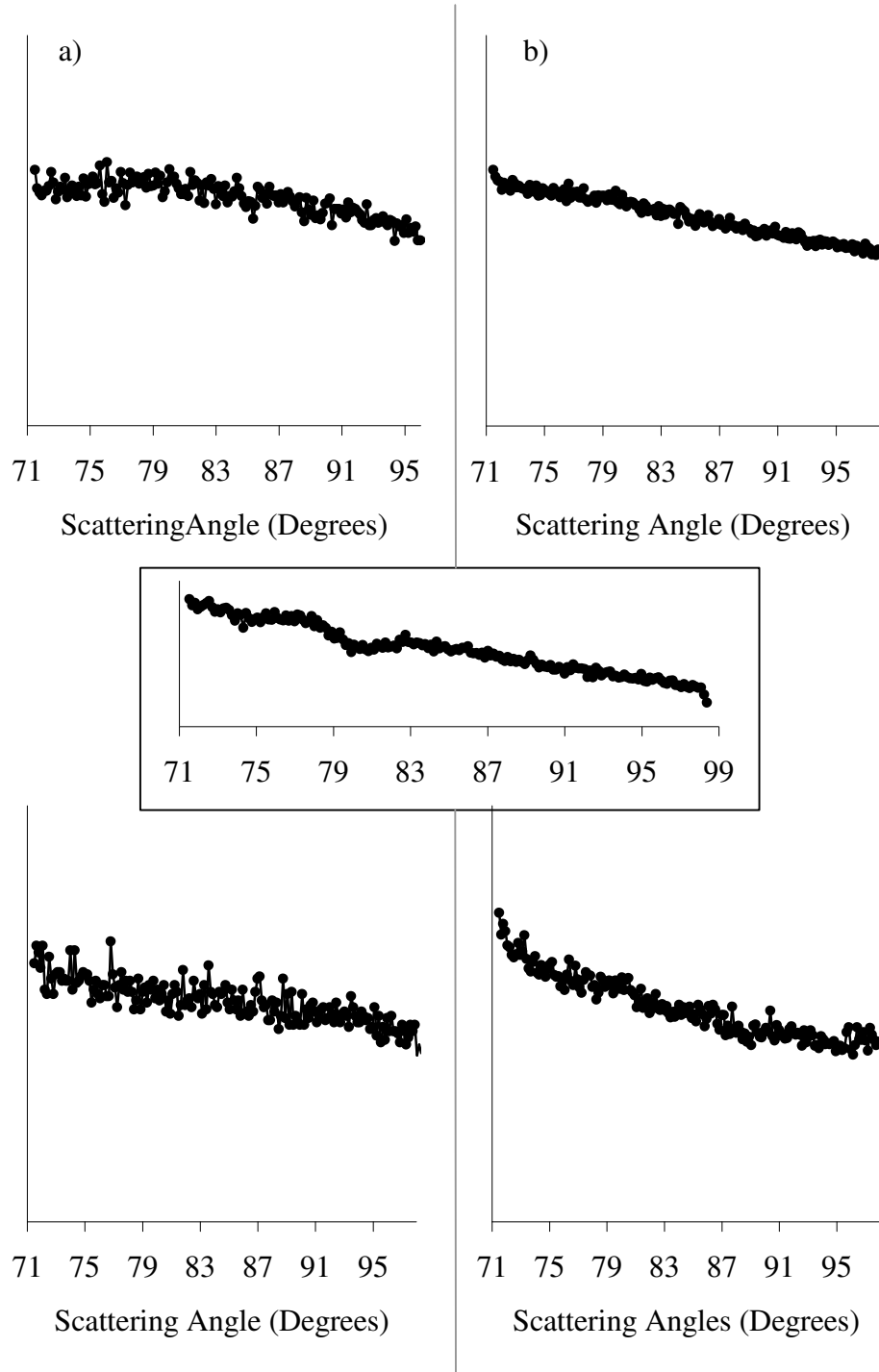


Figure 7.9: Scattering cross section through the Ho (top) and Fe (bottom) signals of spectra shown in Figure 7.8. a) As deposited b) After anneal to ~ 550 °C. Inset: The scattering curve through the Ho signal before Fe deposition. The lack of blocking features in the Ho and Fe signals indicate a lack of order at the surface.

7.4 Conclusion

Preliminary studies into the unique surface of the two dimensional rare earth silicides have been made. The electronic structure of the surface has been investigated by means of scanning tunnelling spectroscopy. The spectroscopy is unusual in that it has not been possible to distinguish between spectra from atomically resolved inequivalent sites. This indicates a delocalised state near the Fermi energy of the surface. The spectra obtained are in qualitative agreement with experimentally and theoretically determined band structures of rare earth silicides and offer a rare opportunity to confirm theoretical predictions regarding the band structure of the empty states.

The use of the surface as a growth template has also been examined. Fe silicides have possible applications in spintronics but their use is hampered by the rough silicide–silicon interface. The possibility that the rare earth layer may act as a form of buffer and the 1×1 surface atomic arrangement a better growth template presents itself. To investigate this an initial MEIS study of Fe growth on Ho 2D silicide was performed. Unfortunately the Fe was seen to disrupt the silicide surface and no ordered structure was obtained. There is however the possibility that oxygen contamination played some role in this disruption. Oxygen is known to disrupt the 2D silicide structure [26]. Further investigation of the use of the 2D silicides as a growth template for Fe is therefore merited.

References

1. D. J. Spence, S. P. Tear, P. Bailey and T. C. Q. Noakes, *Private Communication*
2. H. Kitayama, S. P. Tear, D. J. Spence and T. Urano, *Surf. Sci.* **482-485** 1481 (2001)

3. D. J. Spence, T. C. Q. Noakes, P. Bailey and S. P. Tear, *Surf. Sci.* **512** 61 (2002)
4. L. Stauffer, A. Mharchi, C. Pirri, P. Wetzel, D. Bolmont, G. Gewinner and C. Minot, *Phys. Rev. B* **47** 10555 (1993)
5. C. Rogero, C. Polop, L. Magaud, J. L. Sacedón, P. L. de Andrés and J. A. Martín-Gago, *Phys. Rev. B* **66** 235421 (2002)
6. P. Wetzel, C. Pirri, P. Paki, D. Bolmont and G. Gewinner, *Phys. Rev. B* **47** 3677 (1993)
7. M. Lohmeier, W. J. Huisman, G. ter Horst, P. M. Zagwijn, E. Vlieg, C. L. Nicklin and T. S. Turner, *Phys. Rev. B* **54** 2004 (1996)
8. D. J. Spence, S. P. Tear, T. C. Q. Noakes and P. Bailey, *Phys. Rev. B* **61** 5707 (2000)
9. O. Sakho, F. Sirotti, M. Desantes, M. Sachhi and G. Rossi, *Appl. Surf. Sci.* **56-58** 568 (1992)
10. S. Vandré, T. Kalka, C. Preinesberger and M. Dähne-Prietsch, *J. Vac. Sci. Technol. B* **17** 1682 (1999)
11. S. Vandré, T. Kalka, C. Preinesberger and M. Dähne-Prietsch, *Phys. Rev. Lett.* **82** 1927 (1999)
12. J.-Y. Veuillen, D. B. B. Lollman, T. A. N. Tan and L. Magaud, *Appl. Surf. Sci.* **65/66** 712 (1993)
13. C. Rogero, C. Koitzsch, M. E. González, P. Aebi, J. Cerdá and J. A. Martín-Gago, *Phys. Rev. B* **69** 045312 (2004)

14. J.-Y. Veuillen, L. Magaud, D. B. B. Lollman and T. A. N. Tan, *Surf. Sci.* **269/270** 964 (1992)
15. R. Hofmann and F. P. Netzer, *Phys. Rev. B* **43** 9720 (1991)
16. P. Wetzel, C. Pirri, P. Paki, J. C. Peruchetti, D. Bolmont and G. Gewinner, *Solid State Commun.* **82** 235 (1992)
17. C. J. Chen, *J. Vac. Sci. Technol. A* **6** 319 (1988)
18. N. D. Lang, *Phys. Rev. B* **34** 5947 (1986)
19. R. M. Feenstra, *J. Vac. Sci. Technol. B* **7** 925 (1989)
20. M. J. Hadley, Doctorial Thesis, *Physics, University of York* (1993)
21. P. Mårtensson and R. M. Feenstra, *Phys. Rev. B* **39** 7744 (1989)
22. Ph. Avouris and I. -W. Lyo, *Studying surface chemistry atom-by-atom using the scanning tunneling microscope*, in *Chemistry and Physics of Solid Surfaces*, p. 371, Springer-Verlag: Berlin (1990)
23. R. M. Tromp, R. J. Hamers and J. E. Demuth, *Science* **234** 304 (1986)
24. R. J. Hamers, R. M. Tromp and J. E. Demuth, *Phys. Rev. Lett.* **56** 1972 (1986)
25. P. Wetzel, S. Saintenoy, C. Pirri, D. Bolmont, G. Gewinner, T. P. Roge, F. Palmino, C. Savall and J. C. Labrune, *Surf. Sci.* **355** 13 (1996)
26. D. J. Spence and S. P. Tear, *Personal Communication* (2004)